

Measurements of Air Blast Pressure Waves using Pencil Probes

Petr DVORÁK^{1*}, Eva ZEZULOVÁ¹

¹Department of Engineer Technologies, Faculty of Military Technologies, University of Defence, Address: Kounicova 65, 662 10 Brno, Czech Republic

Correspondence: [*petr.dvorak@unob.cz](mailto:petr.dvorak@unob.cz)

Abstract

The article deals with measurements of air blast pressure waves using pencil probes. The pressure waves from explosive detonations were recorded using pencil probes in different setups, arrangements, and at multiple standoff distances. Another step is to get data from measurements to be used in other applications. Several blast parameters are presented as a baseline for further analysis (peak overpressure, rise time, positive-phase duration, impulse). The approach should support later comparison and uncertainty assessment with analytical data.

KEY WORDS: *air blast, pressure waves, pencil probes, peak overpressure, positive impulse*

Citation: Dvořák, P.; Zezulová, E. Measurements of Air Blast Pressure Waves using Pencil Probes. In Proceedings of the Challenges to National Defence in Contemporary Geopolitical Situation, Brno, Czech Republic, 7-10 September 2026. ISSN 2538-8959, <https://doi.org/10.47459/cndcgs.2026.3>

1. Introduction

The topic of pressure waves created by explosions in the air is very important in protective design, hazard evaluation, and in the validation of numerical or analytical models. Engineering conclusions often rely on only a few basic descriptors of the pressure waveform, such as the peak overpressure, the impulse, and the duration of the positive phase. However, it is necessary to note that these quantities may change significantly due to different factors, for example the standoff distance or the position of the explosive source. In field experiments, pressure records are usually obtained with compact sensors known as pencil probes. These sensors are appreciated because they are easy to transport, can be arranged in various arrays, and can be quickly relocated for different test setups. At the same time, blast waves from a detonation have very steep leading edges and very short characteristic times, which makes it difficult to achieve accurate measurements in real testing conditions. The recorded peak value and rise time can be affected by several elements, including the bandwidth of the sensor, the sampling frequency, the mounting configuration, and the flow conditions around the transducer.

Another difficulty in outdoor experiments is the effect of ground reflection. When the charge is placed directly on the ground, the spherical incident wave interacts with the surface and creates a reflected wave. Depending on the geometry and distance, this reflected component may significantly increase the overpressure at the measurement location. As a result, both the shape of the observed waveform and the values derived from it can be altered. It is therefore important to take this into account when comparing experimental data with ideal analytical equations.

Currently an ongoing effort is focused on the measurement and analysis of air blast detonations using several sensor standoff distances. Pressure time histories are recorded with pencil probes installed on tripods or wooden stands in different arrangements, usually including several measuring points depending on the specific test series. The current aim is to develop a replicable workflow that can transform raw measurements into a consistent set of blast parameters and prepare the data for quantitative comparison with analytical calculations. The emphasis at this stage is on the right approach, on quality control, and on defining the comparison strategy that will allow reliable conclusions after the full parameter study and uncertainty analysis are completed.

For this reason, the evaluation of pencil probe measurements requires a systematic procedure that considers both experimental and signal processing aspects. Attention must be paid to pressure sensor orientation, probe positioning, triggering accuracy, and the repeatability of individual tests. In addition, the treatment of raw pressure records, including

baseline correction, filtering, and identification of relevant waveform features, has a direct influence on the resulting blast parameters.

2. Method of Investigation

The experimental data were obtained during repeated outdoor detonation tests, with the explosive charge positioned directly on the terrain. This placement represents a practical surface-burst condition in which the incident blast wave interacts with the ground and generates a reflected component that can partially merge with the incident waveform at the measurement locations (Fig. 1). Pencil probes were deployed in configurable arrays covering several standoff distances. Each test employed between 3 and 15 measurement stations, typically arranged along one or more radial lines from the source to support trend evaluation dependent on distance. Probes were mounted on tripods or wooden stands (Fig. 2, Fig. 3) to enable rapid setup and reconfiguration. The mounting height and orientation were kept as consistent as practicable, with sensors oriented toward the source and positioned to reduce immediate shielding or scattering by nearby objects such as vegetation or uneven terrain.

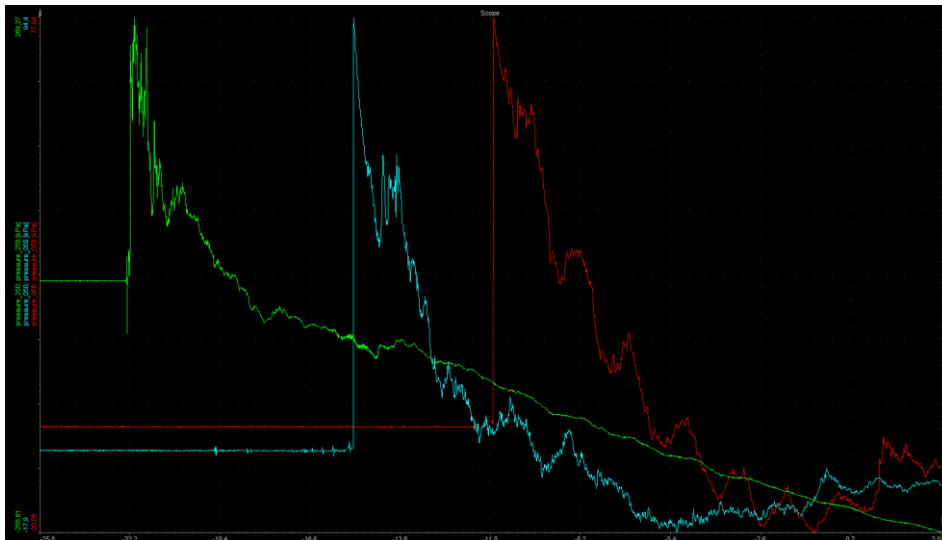


Fig. 1. Time series plot of overpressure measured by three pencil probes obtained from data acquisition software.

The acquisition system recorded all channels synchronously at 200 kHz, providing a 5 μ s sampling interval. Each record included a pre-event window used to estimate baseline pressure, drift, and noise statistics, followed by a post-event window long enough to capture the full positive phase and any secondary features associated with ground reflection. Prior to analysis, signals were screened for quality issues such as clipping or saturation, channel dropouts, and anomalous offsets. Triggering was performed by the acquisition system. For each test, configuration metadata were compiled when available, including station identifiers, measured standoff distances, stand type, approximate probe elevation, and brief environmental notes (wind and terrain condition), to support grouping of comparable shots and assessment of different measurements parameters.



Fig. 2. Different types of fixations – wooden poles.



Fig. 3. Different types of fixations – tripods.

3. Blast Parameters

In order to compare pressure wave records obtained at different setups and probes, and during different test series, each pressure trace is reduced to a small set of reproducible descriptors that capture:

- Timing – when the wave arrives.
- Amplitude – how large the peak is.
- Loading severity – how long the pressure remains positive and how much total area it delivers.

The extraction procedure therefore begins with baseline referencing to remove the ambient pressure level and ends with a consistent definition of the positive phase, so that peak values and integrals are evaluated over comparable windows. Because outdoor surface-burst tests may contain secondary features such as ground reflections, the definitions used for arrival time and positive phase termination are stated explicitly and applied identically to all channels. The resulting parameter set provides a compact representation that supports trend analysis versus distance and objective comparison with analytical predictions:

- Overpressure is the baseline pressure used for all subsequent descriptors. It removes the static ambient level and highlights the transient loading. It is computed from a pre-event window to ensure consistent comparison across stations and test campaigns.

$$\Delta p(t) = p(t) - p_0 \quad (1)$$

where: $\Delta p(t)$ – overpressure; $p(t)$ – measured absolute pressure; p_0 – baseline/ambient pressure; t – time.

- Arrival time marks when the wavefront reaches a sensor and it is essential for propagation analysis and time alignment. A noise-referenced threshold definition is robust in field data and minimizes false triggers.

$$t_a = \min\{t: \Delta p(t) \geq k \sigma_0\} \quad (2)$$

where: t_a – arrival time; $\Delta p(t)$ – overpressure; k – threshold multiplier; σ_0 – standard deviation of pre-event overpressure; t – time.

- Peak overpressure is the maximum positive value of $\Delta p(t)$ and is one of the most commonly reported blast parameters. It can be sensitive to bandwidth and mounting, so the extraction definition should be stated explicitly.

$$\Delta p_{\max} = \max_t \Delta p(t) \quad (3)$$

where: Δp_{\max} – peak overpressure; $\Delta p(t)$ – overpressure; \max_t – maximum over time t .

- Rise time describes the effective steepness of the wavefront and is typically defined using fractional levels of the peak to reduce sensitivity to small oscillations at the very start of the front. The 10–90% definition is widely used for repeatability across records.

$$t_r = t_{90} - t_{10} \quad (4)$$

where: t_r – rise time; t_{10} – time when $\Delta p(t) = 0.1\Delta p_{\max}$ (first crossing after arrival); t_{90} – time when $\Delta p(t) = 0.9\Delta p_{\max}$.

- Positive phase duration quantifies how long the overpressure remains above ambient after arrival; it is important for waveform idealization and for comparing explosions at different standoffs. In reflection-influenced records, the rule for selecting t_0 should be consistent to avoid bias in duration and impulse.

$$t_+ = t_0 - t_a \quad (5)$$

where: t_+ – positive-phase duration; t_0 – first return-to-ambient (or first zero crossing) after arrival; t_a – arrival time.

- Positive impulse is the time integral of overpressure over the positive phase and represents the total loading per unit area. Compared with peak pressure, impulse is often more stable when the leading edge is affected by bandwidth limits.

$$I_+ = \int_{t_a}^{t_a+t_+} \Delta p(t) dt \quad (6)$$

where: I_+ – positive impulse; $\Delta p(t)$ – overpressure; t_a – arrival time; t_+ – positive-phase duration; dt – time increment.

- Friedlander-type positive-phase approximation provides a compact analytical description of the positive phase and is useful for fitting and comparing waveform shape in addition to peak and impulse. The coefficient b controls the decay rate and is typically obtained by least-squares fitting over the positive phase.

$$\Delta p(t) = \Delta p_{\max} \left(1 - \frac{t}{t_+}\right) e^{\left(-b \frac{t}{t_+}\right)}, 0 \leq t \leq t_+ \quad (7)$$

where: $\Delta p(t)$ – overpressure (positive phase); Δp_{\max} – peak overpressure; t_+ – positive-phase duration; b – decay coefficient; t – time measured from arrival within the positive phase.

The above-mentioned equations are aimed at converting each measured pressure probe measurement into a compact, comparable set of blast descriptors. Starting from baseline-referenced overpressure $\Delta p(t)$, then it identifies arrival time t_a using a noise-scaled threshold, then extracts peak overpressure Δp_{\max} , rise time t_r , positive-phase duration t_+ , and positive impulse I_+ by integrating $\Delta p(t)$ over the positive phase. This parameter set enables objective validation of analytical models by comparing predicted and measured peaks, impulses, and arrival times using error metrics or parity plots. Finally, the dataset can be extended into products focused on applications, such as envelopes describing pressure and impulse for loading classification, or screening criteria for identifying tests dominated by reflection and limitations related to sensors

4. Investigation Results

At the present stage, the main outcome is the development of a robust extraction pipeline together with a set of indicators, which are used to decide which records are appropriate for parameters comparison. In the current standoff range, the pressure time series show the expected blast wave shape:

- A rapid increase close to the arrival.
- A peak overpressure.
- And a positive phase that declines with time.

Peak overpressure and impulse are generally reliable, if signal cutting is not present and that baseline drift is sufficiently controlled. The rise time remains the most sensitive descriptor as it depends strongly on the steepness of the incident front and on the effective bandwidth of the measurement chain, and it may also be affected by the type of sensor mounting or flow effects near to the ground.

5. Conclusions

This work defines a background for converting pencil probe measurements of detonation driven by air blast waves into a dataset suitable for analytical assessment. The workflow includes baseline correction, arrival time detection, bandwidth preprocessing, and standardized parameter extraction – peak, rise time, positive duration, impulse. The data series with varying standoff distances reflects practical field conditions with ground reflection due to the contact with terrain. With the data assessment still ongoing, the developed methodology establishes the basis for reporting reproducible parameter trends.

The major limitation is the combined influence of transducer dynamics and field mounting on the steep leading edge of the blast waveform. At the current sampling, gross waveform features are resolved, but very sharp rise time behavior may not be fully captured in the near field, and mounting on tripods or wooden stands can introduce vibration and alignment variability. Second, ground reflection is naturally dependent on geometry and terrain. Third, outdoor environmental conditions such as wind or temperature gradients can alter waveform shape and complicate comparability between probes.

Acknowledgements. This work was prepared with the support of the Ministry of Defence of the Czech Republic, Partial Project for Institutional Development, AirOps – Conduct of airspace operations.

References

1. **Charles N Kingery, Gerald Bulmash.** Airblast Parameters from TNT Spherical Air Burst and Hemispherical Surface Burst. Picatinny Arsenal Technical Report ARBRL-TR-02555, 1984.
2. Kingery-Bulmash Blast Parameter Calculator. International Ammunition Technical Guidelines IATG 01.80. 2021.
3. **Vasilis Karlos, George Solomos, Martin Larcher.** Analysis of blast parameters in the near-field for spherical free-air explosions. Technical report by the Joint Research Centre. 2016.
4. **Skriudalen, S., Skjold, A., Hugsted, B., Teland, J. A., & Huseby, M.** Misalignment Effects Using Blast Pencil Probes. Norwegian Defence Research Establishment (FFI) 2014, ISBN 978-82-464-2343-2.
5. **Isaac, O. S., Alshammari, O. G., Pickering, E. G., Clarke, S. D., & Rigby, S. E.** Blast wave interaction with structures – An overview. *International Journal of Protective Structures*, 2023, 14(4), 584–630. Available online: <https://doi.org/10.1177/20414196221118595>.
6. **Wei, T., Hargather, M. J.** A new blast wave scaling. *Shock Waves*, 2021, 31, 231–238. Available online: <https://doi.org/10.1007/s00193-021-01012-y>.
7. **Tasissa, A. F., Hautefeuille, M., Fitek, J. H., Radovitzky, R. A.** On the formation of Friedlander waves in a compressed-gas-driven shock tube. *Proceedings of the Royal Society A*, 2016, 472(2186), 20150611. Available online: <https://doi.org/10.1098/rspa.2015.0611>.
8. **Cook, A. W., Bauer, J. D., Spriggs, G. D.** The reflection of a blast wave by a very intense explosion. *Proceedings of the Royal Society A*, 2021, 477(2250), 20210154. Available online: <https://doi.org/10.1098/rspa.2021.0154>.
9. **Karlos, V., Solomos, G., Larcher, M.** Analysis of the blast wave decay coefficient using the Kingery–Bulmash data. *International Journal of Protective Structures*, 7(3), 2016, 409–429. Available online: <https://doi.org/10.1177/2041419616659572>.
10. **Bagabir, A. M.** Numerical simulations of the impact of reflective surfaces on blast propagation and urban safety. *Journal of Umm Al-Qura University for Applied Sciences*. Available online: <https://doi.org/10.1007/s43994-025-00288-5>.

Disclaimer/Publisher’s Note: The statements, opinions and data contained in all publications are solely those of the individual author(s) and contributor(s) and not of CNDCGS 2026 and/or the editor(s). CNDCGS 2026 and/or the editor(s) disclaim responsibility for any injury to people or property resulting from any ideas, methods, instructions or products referred to in the content.